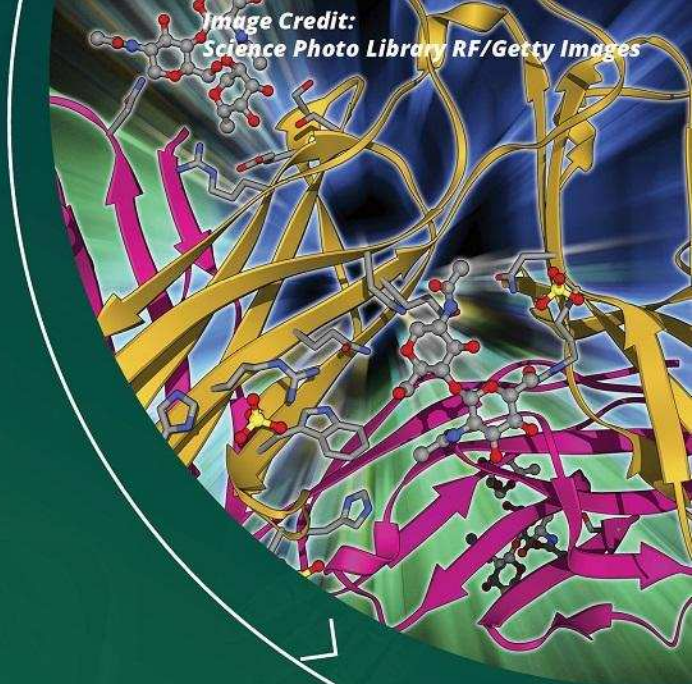
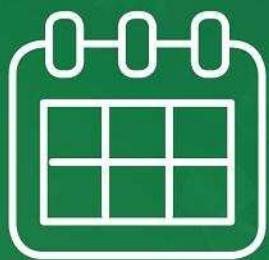


Join our webinar



Cell-based immunotherapies: T-Cell CARs

Now Available
On Demand







Register Here

invitrogen
by Thermo Fisher Scientific

**CURRENT
PROTOCOLS**
A Wiley Brand

WILEY

AQP2 can modulate the pattern of Ca²⁺ transients induced by store-operated Ca²⁺ entry under TRPV4 activation

Alejandro Pizzoni^{1,2}  | Macarena López González¹ | Gisela Di Giusto^{1,2} |
Valeria Rivarola^{1,2}  | Claudia Capurro^{1,2}  | Paula Ford^{1,2} 

¹Laboratorio de Biomembranas, Facultad de Medicina, Departamento de Ciencias Fisiológicas, Universidad de Buenos Aires, Buenos Aires, Argentina

²CONICET-Universidad de Buenos Aires, Instituto de Fisiología y Biofísica “Bernardo Houssay” (IFIBIO), Buenos Aires, Argentina

Correspondence

Prof. Paula Ford, PhD, Laboratorio de Biomembranas, IFIBIO Houssay, CONICET-UBA, Facultad de Medicina, Departamento de Ciencias Fisiológicas, Universidad de Buenos Aires, Paraguay 2155, piso 7 (1121) Buenos Aires, Argentina.
Email: pford@fmed.uba.ar

Funding information

Universidad de Buenos Aires (UBA, <http://www.uba.rec.ar>), Grant number: UBACYT 20020130100697BA 2014-2017; Consejo Nacional de Investigaciones Científicas y Técnicas (www.conicet.gov.ar), Grant number: CONICET PIP/0227, 2011; Fondo Nacional para la Ciencia y la Tecnología (FONCYT, <http://www.agencia.gov.ar>), Grant number: PICT/0750, 2012

Abstract

There is increasing evidence indicating that aquaporins (AQPs) exert an influence in cell signaling by the interplay with the TRPV4 Ca²⁺ channel. Ca²⁺ release from intracellular stores and plasma membrane hyperpolarization due to opening of Ca²⁺-activated potassium channels (KCa) are events that have been proposed to take place downstream of TRPV4 activation. A major mechanism for Ca²⁺ entry, activated after depletion of intracellular Ca²⁺ stores and driven by electrochemical forces, is the store-operated Ca²⁺ entry (SOCE). The consequences of the interplay between TRPV4 and AQPs on SOCE have not been yet investigated. The aim of our study was to test the hypothesis that AQP2 can modulate SOCE by facilitating the interaction of TRPV4 with KCa channels in renal cells. Using fluorescent probe techniques, we studied intracellular Ca²⁺ concentration and membrane potential in response to activation of TRPV4 in two rat cortical collecting duct cell lines (RCCD₁), one not expressing AQPs (WT-RCCD₁) and the other transfected with AQP2 (AQP2-RCCD₁). We found that AQP2 co-immunoprecipitates with TRPV4 and with the small-conductance potassium channel (SK3). We also showed that AQP2 is crucial for the activation of SK3 by TRPV4, leading to hyperpolarization of the plasma membrane. This seems to be relevant to modulate the magnitude of SOCE and is accompanied by TRPV4 translocation to the plasma membrane only in AQP2 expressing cells. These findings open the perspective to further investigate whether the interplay between different AQPs with TRPV4 and KCa channels can be an important mechanism to modulate SOCE with physiological relevance.

KEYWORDS

aquaporin 2, KCa, membrane potential, store operated calcium entry, TRPV4

1 | INTRODUCTION

There is a growing body of evidence indicating the involvement of aquaporins water channels (AQPs) in numerous cellular processes, apparently not only related to their canonical function of water permeation, with important

implications in physiological and pathological processes.¹ For instance, AQPs have been demonstrated to have a role in cell volume regulation, migration, apoptosis, cell proliferation, angiogenesis and tumor growth, although the involved mechanisms are not well understood.^{1–3} Presumably, in these processes, AQPs may exert an influence in cell signaling by

different mechanisms such as crosstalk with other cell membrane proteins or by forming macromolecular complexes.^{1,2} There is increasing evidence about the interplay between AQPs and the TRPV4 non selective Ca^{2+} channel, a member of the transient receptor potential (TRPs) family in cell volume regulation. The role of Ca^{2+} as a triggering signal of cell regulatory volume decrease (RVD) mechanisms is still a matter of debate since RVD is Ca^{2+} -dependent in some cell types^{4,5} and Ca^{2+} -independent in others.^{6,7} Several studies, including ours, reported evidence that activation of TRPV4 by hypotonic stimulus is influenced by the presence of AQPs, and it is responsible for Ca^{2+} entry which, in turn, triggers RVD mechanisms.^{4,8,9} In salivary glands TRPV4 and AQP5 are functional and physically associated, probably via indirect interactions.⁴ In renal cells we described a functional interaction between AQP2 and TRPV4, however, we did not perform co-immunoprecipitation experiments to rule out some type of physical interaction.⁹ Benfenati et al⁸ proposed that TRPV4-dependent regulation of osmotic fluxes within the astrocyte end foot requires an obligatory physical interaction with AQP4. In the same way, Jo et al¹⁰ described a TRPV4-AQP4 interaction that influences cell volume regulation as well as Ca^{2+} signaling in retinal Müller glia. Interestingly, this work proposes that AQP4 does not modify TRPV4 currents directly but “secondary components of TRPV4-dependent Ca^{2+} homeostasis” would be affected, such as ATP release, Ca^{2+} release from internal stores, and/or activation of store-operated channels (SOCs). However, the role of AQPs in these linked signaling processes has not been studied.

Store-operated Ca^{2+} entry (SOCE) is a major mechanism for Ca^{2+} influx in many cell types. SOCE plays a homeostatic role in providing Ca^{2+} to refill intracellular Ca^{2+} stores after Ca^{2+} has been released. Importantly, Ca^{2+} entry through SOCs also functions as a key signal to regulate diverse cellular processes including migration, proliferation or apoptosis that are processes in which different AQPs and TRPs have been informed as being involved.^{1,11–14} A previous work from our laboratory revealed that in cortical collecting duct cells, strong osmotic shocks, elicits intracellular Ca^{2+} ($[\text{Ca}^{2+}]_i$) transients analogous to SOCE only in cells expressing AQP2.⁵ This study was performed using two rat cortical collecting duct cell lines (RCCD₁), one not expressing AQPs (WT-RCCD₁) and the other transfected with AQP2 (AQP2-RCCD₁). Although the two cell lines responded differently to hypotonicity, both lines have the machinery to generate SOCE. We also showed that hypotonic stimulation only enriches TRPV4 in the membrane of cells expressing AQP2.⁹ Interestingly, in isosmotic conditions we found that AQP2 expression accelerates the proliferation rate of RCCD₁ cells¹⁵ a process that is sensitive to the TRPV channel antagonist, ruthenium red.¹² Therefore, it could be that AQP2, together with TRPV4, may play a role in modulating SOCE.

The participation of TRPV4 in mechano- and osmotransduction contributes to important functions including cellular and systemic volume homeostasis, arterial dilation, nociception, epithelial hydroelectrolyte transport, bladder voiding, ciliary beat frequency regulation, and in flow-mediated K^+ secretion.^{8,14,16} Studies in several cells and tissues established that influx of Ca^{2+} via TRPV4 channels would lead to the local activation of different Ca^{2+} -activated potassium channels (KCa).^{17–19} Recently, it has been demonstrated in native mouse cortical collecting ducts (CCD), that selective activation of TRPV4 channel, induces Ca^{2+} influx that, in turn, activates KCa channels leading to hyperpolarization of the plasma membrane.²⁰

Since SOCE is an electrogenic process, hyperpolarization can enhance Ca^{2+} influx and therefore, we hypothesize that by modulating TRPV4 activity, AQP2 can affect KCa channels and in consequence $[\text{Ca}^{2+}]_i$ transients induced by SOCE. Recently, it has been proposed that sustained $[\text{Ca}^{2+}]_i$ elevations via SOCE are required for adequate AQP2 trafficking and expression.²¹ Physiological changes in membrane AQP2 expression occur during the transition from diuresis to antidiuresis state. These changes occur with variations in osmolarity and in the rate of flow that are important stimuli for TRPV4 activation thus, understanding the role played by AQP2 and TRPV4 in SOCE is especially interesting in the case of cortical collecting duct cells. Therefore, the aim of our study was to test the hypothesis that AQP2 can modulate SOCE by facilitating the interaction of TRPV4 with KCa channels.

Using fluorescent probe techniques, we studied $[\text{Ca}^{2+}]_i$ and membrane potential (V_m) changes in response to specific activation of TRPV4, with the agonist 4α -PDD, in WT-RCCD₁ and AQP2-RCCD₁. The data here presented demonstrate, for the first time, that the presence of AQP2 is crucial for the activation of the high Ca^{2+} -binding affinity small-conductance K^+ (SK) channel by TRPV4, leading to hyperpolarization of the plasma membrane. This process seems to be relevant to modulate the magnitude of SOCE in RCCD₁ cells and is accompanied by TRPV4 translocation to the plasma membrane only in AQP2 expressing cells. In addition, we found that AQP2 co-immunoprecipitate with SK3 and TRPV4 channels and after Ca^{2+} store depletion, AQP2 colocalizes with SK3 and TRPV4 at the plasma membrane.

2 | MATERIALS AND METHODS

2.1 | Cell culture

WT-RCCD₁ cells (not expressing AQPs) were grown in modified DM medium (Dulbecco's modified Eagle's medium/Ham's F-12

1:1 v/v, 14 mM NaHCO₃, 3.2 mM glutamine, 5 × 10⁻⁸ M dexamethasone, 3 × 10⁻⁸ M sodium selenite, 5 µg/mL insulin, 10 µg/mL epidermal growth factor, 5 × 10⁻⁸ M triiodothyronine, 10 U/mL penicillin + streptomycin, 20 mM Hepes; pH 7.4) and 2% fetal bovine serum (FBS) Gibco (Thermo Fisher Scientific, Whitby, Canada).^{22,23}

AQP2-RCCD₁ cells, stably transfected with cDNA coding for rat AQP2, (constitutively expressing AQP2 in the apical plasma membrane) were maintained in the same medium containing Geneticin (400 µg/mL, Life Technologies, Palo Alto, CA) as previously reported.²⁴

Cells were maintained at 37°C and in 5% CO₂ during culture. All experiments were performed at 20°C on subconfluent cells, between the 20th and 40th passages, grown on coverslips during 2 or 3 days.

2.2 | Intracellular Ca²⁺ measurement

WT- and AQP2-RCCD₁ cells were incubated in 10 µM Fura-2 acetoxymethyl ester (Fura-2 AM) Molecular Probes, Thermo Fisher Scientific (Eugene, OR) for 60 min at 37°C and then washed to remove the excess of dye. To prevent dye compartmentalization upon loading, 0.2% Pluronic F-127 (Molecular Probes) was used to dissolve the Fura-2 AM dye. The coverslips were placed at 20°C in the dark and incubated in the experimental buffer for 15 min before the experiments. Ca²⁺ measurements were made using a TE-200 epifluorescence inverted microscope (Nikon, Japan) connected to an ORCA-100 CCD camera (model C4742-95, Hamamatsu Photonics, Japan). Fluorescence emission at 510 nm was monitored while alternating between 340 and 380 nm excitation wavelengths at a frequency of 0.1 Hz, using the Metafluor acquisition program (Universal Imaging Corporation, West Chester, PA). Intracellular Ca²⁺ measurements are shown as 340/380 nm ratios (R_i) normalized to initial values (R_i/R₀). All experiments were corrected for background fluorescence before the Fura-2 ratio was calculated.

Starting from a constant baseline level, the increase in [Ca²⁺]_i was analyzed as the area under the curve (AUC) during the first 10 or 20 min (depending on the experiment type) and the initial slope of the [Ca²⁺]_i increase during the first minute following each intervention. Slopes and AUCs, two parameters widely used to quantify Ca²⁺ signals, were calculated using GraphPad Prism 6 software (GraphPad Software, San Diego, CA).

2.3 | Measurement of membrane potential changes

Transmembrane potential was evaluated using the potential-sensitive dye, bis-(1,3-dibutylbarbituric acid) trimethine oxonol [DiBAC₄(3)]. Cells were loaded with 2.5 µM DiBAC₄(3) for 20 min at 20°C, and placed on the stage of the same microscope described in the previous section.

Fluorescence emission at 520 nm was monitored with a 490 nm excitation wavelength at a frequency of 0.1 Hz. Fluorescence intensity was monitored until it reached a stable value before starting the experiments and changes after interventions were relativized to stationary values (F_i/F₀). The fluorescence changes acquired with DiBAC₄(3) in WT- and AQP2-RCCD₁ cells were calibrated by adding 5 µM of the ionophore gramicidin to solutions containing different concentrations of NaCl replaced with N-Methyl-D-glucamine chloride (NMDGCl) in an equimolar way to maintain osmolarity (Figures 1A and 1B). Four extracellular NaCl concentrations were tested; 90, 60, 30, and 0 mM corresponding to membrane potentials of -4.4, -14, -29.6, and -74.3 mV, respectively. V_m was calculated as:

$$V_m = \frac{RT}{F} \ln[(Na_o + K_o)/(Na_i + K_i)] \quad (1)$$

Intracellular concentrations of Na⁺ and K⁺ were assumed to be 19 and 95 mM, respectively based on the values reported for renal cells. A positive linear regression was obtained for each cell line (Figures 1C and 1D). WT- and AQP2-RCCD₁ cells show analogous V_m values in basal conditions (WT: -37.2 ± 2.9 mV vs AQP2: -42.01 ± 1.26, n = 75, N = 3; NS) and a 1% change in fluorescence corresponds to a similar V_m variation in both cell lines (WT: 1.9 ± 0.2 mV vs AQP2: 2.1 ± 0.4 mV n = 75, N = 3; NS). Moreover, both cell lines respond in a comparable way when cells were exposed 3 min to a depolarizing condition with a high extracellular K⁺ solution (95 mM) (WT: -9.0 ± 4.9 mV vs AQP2: -11.0 ± 3.6 mV, n = 75, N = 3; NS).

2.4 | Immunoprecipitation and immunoblotting experiments

For immunoprecipitation studies anti-AQP2 (Santa Cruz Biotechnology, Dallas, TX, Cat# sc-9882, RRID: AB_2289903), anti-TRPV4 (Alomone Labs, Jerusalem, Israel, Cat# ACC-034, RRID: AB_2040264), and anti-SK3 (Alomone Labs, Cat# APC-025, RRID: AB_2040130) antibodies were covalently coupled to M-280 Tosylactivated Dynabeads (Invitrogen, Thermo Fisher Scientific, Carlsbad, CA). Coated beads were then incubated with WT or AQP2-RCCD₁ cell lysates for 1 h at 37°C with tilting and rotation. After washing with phosphate-buffered saline, the beads were resuspended in sample buffer, and the target protein bound was eluted by boiling for 5 min. Immunoblotting experiments were carried out as previously described.⁹ Proteins were separated in 7.5% SDS-polyacrylamide electrophoresis minigels using the Tris-Tricine buffer system and then transferred to nitrocellulose membranes (Mini Protean II, Bio-Rad, Mississauga, Canada). Blots were blocked with 1% BSA (Sigma-Aldrich, St. Louis, MO) and then probed using either anti-SK3 (dilution 1/1000), anti-TRPV4 (dilution 1/1500), or anti-AQP2 (dilution 1/250, Santa Cruz

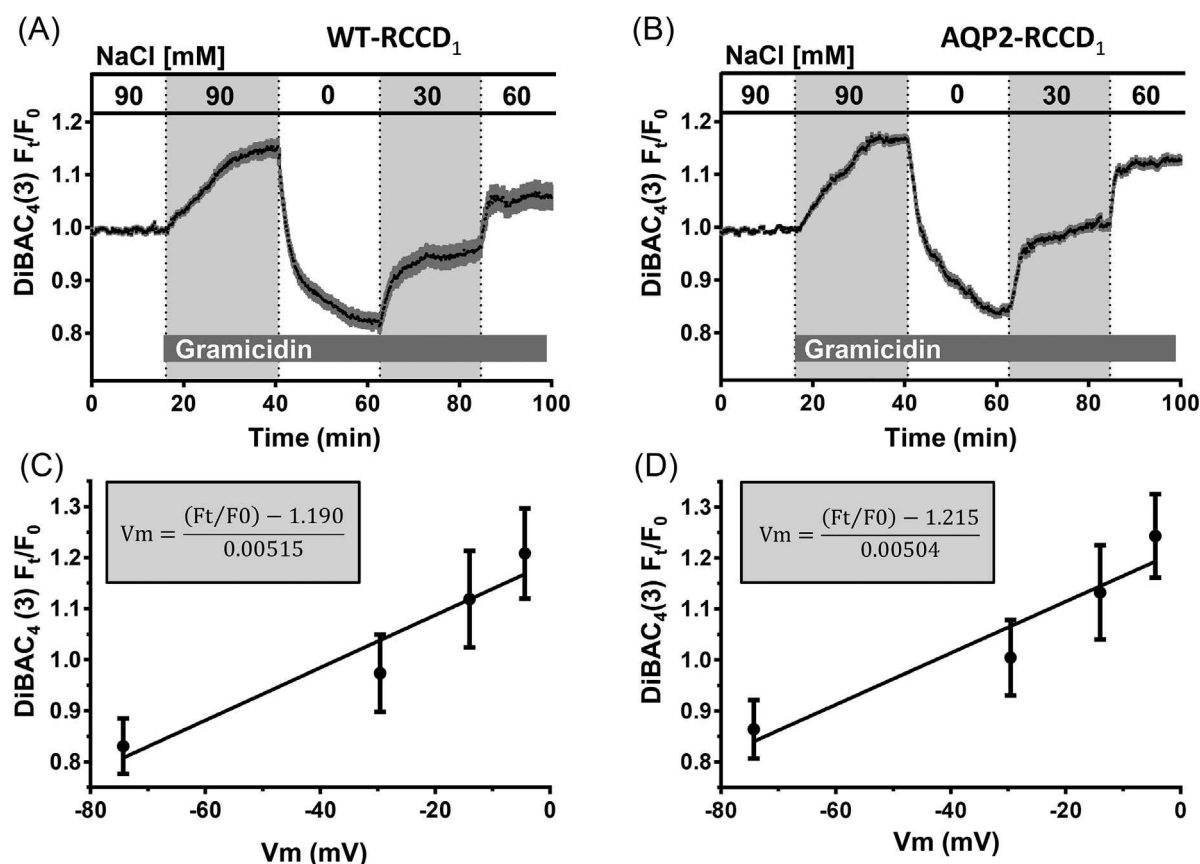


FIGURE 1 Calibration of voltage sensitive dye DiBAC₄(3) in RCCD₁ cells. A and B, Representative experiments showing the normalized fluorescence (F_t/F_0) of WT- (A) and AQP2-RCCD₁ (B) cells previously loaded with 2.5 mM DiBAC₄(3). Cells were exposed sequentially to different extracellular concentrations of NaCl (90, 0, 30, and 60 mM) in solutions containing 5 μ M gramicidin. C and D, Normalized fluorescence (F_t/F_0) plotted versus membrane potential (V_m). The lines plotted are the best linear regression from which slopes and y-intercepts were used for each V_m equation (insets). Values are the mean \pm SEM of at least 72 cells from three separate experiments

Biotechnology, Cat# sc-515770 or Santa Cruz Biotechnology, Cat# sc-9882). After being rinsed with PBS-Tween 0.1%, membranes were incubated with the appropriate secondary antibodies (anti-rabbit [Cat# 111-035-144, RRID: AB_2307391], anti-goat [Cat# 705-035-003, RRID: AB_2340390], or anti-mouse [Cat# 115-035-003, RRID: AB_10015289] IgG conjugated to horseradish peroxidase, dilutions 1/10000 or 1/25000) and visualized using the chemiluminescence method (SuperSignal Substrate, Pierce). Images were captured on a G:BOX (Syngene, Frederick, MD).

2.5 | Immunofluorescence studies

Cells were first fixed in 3% paraformaldehyde for 15 min at room temperature and then permeabilized with 0.2% Triton X-100 for 30 min at room temperature. Samples were blocked with 1% bovine serum albumin (BSA, Sigma-Aldrich) and incubated overnight at 4°C with the same primary antibodies previously described; anti-AQP2 (dilution: 1/50), anti-TRPV4 (dilution: 1/1500), and/or anti-SK3 (dilution: 1/100). Then, samples were

washed and incubated with the correspondent secondary antibodies (Jackson ImmunoResearch Labs, West Grove, PA, Cat# 115-165-003, RRID: AB_2338680:1/200; Molecular Probes, Cat# A-11055, RRID: AB_142672:1/100; Molecular Probes, Cat# A-11057, RRID: AB_142581: 1/100) for 2 h at room temperature. To label the plasma membrane, live cells were incubated with 5 μ g/mL Wheat Germ Agglutinin, Alexa Fluor 488 conjugate (WGA-488, Molecular Probes, Cat# W11261) for 30 min at 4°C prior to fixation. Coverslips were mounted with Vectashield (Vector Laboratories, Burlingame, CA) mounting medium.

2.6 | Colocalization digital image acquisition and analysis

Images were acquired and digitalized using an Olympus FV1000 confocal microscope: objective UPlanFI 40X/1.30 NA ∞ /0.17/FN26.5. A minimum of 12 fields from at least three different coverslips were analyzed for each condition.

To obtain a statistical measure of the degree of colocalization between TRPV4 and WGA-488 we used the "Coloc" module of Imaris 7.1.0 software (Bitplane, Switzerland) that implements the Pearson's correlation coefficient (PCC). PCC is a quantitative measurement that estimates the degree of overlap between fluorescence signals obtained in two channels. It takes into consideration only similarity between shapes, while ignoring the intensities of signals. PCC values range from 1, an indication of complete colocalization of two structures; 0, which indicates random correlation; to -1, which indicates complete separation of two signals. This program also implements an automatic thresholding algorithm inspired by the Costes' method for performing colocalization analysis of fluorescence images. The aim of this approach is to determine automatically an intensity threshold for each channel. Pixels below this threshold are ignored for the purposes of the colocalization quantification. The point spread function (PSF) width used for thresholding was overestimated (1 μm) and P -value's obtained were equal to 1 in all cases, indicating a statistically significant correlation.

2.7 | Solutions and chemicals

The experimental buffer contained (in mM): 90 NaCl, 10 NaHCO_3 , 5 KCl, 1 CaCl_2 , 0.8 MgSO_4 , 1 MgCl_2 , 100 mannitol, 20 Hepes, 5 glucose. Ca^{2+} -free solutions were made by adding EGTA (1 mM) and replacing CaCl_2 with MgCl_2 . For high K^+ solutions NaCl was replaced with KCl in an equimolar way to maintain osmolality.

The osmolalities were routinely measured by a vapor pressure osmometer (Vapro 5520, Wescor, Logan, UT). All solutions were titrated to pH 7.40 using Tris (Sigma-Aldrich) and bubbled with atmospheric air.

The following chemicals and stock solutions were used in this study: DiBAC₄(3) (Molecular Probes, 600 μM in DMSO), Fura-2 AM (Molecular Probes, 1 mM in DMSO), Apamin (Tocris, 25 μM in water), Thapsigargin (Molecular Probes, 1.5 mM in DMSO), Gramicidin (Sigma-Aldrich, 10 mM in DMSO), 4-phorbol-12,13-didecanoate (4 α -PDD) (Sigma-Aldrich, 600 μM in DMSO), HC-067047 (Sigma-Aldrich, 20 mM in DMSO), SKF-96365 (Sigma-Aldrich, 20 mM in water), Dantrolene (Sigma-Aldrich, 10 mM in DMSO). Caffeine-containing solutions were prepared by addition of appropriate mass of caffeine (Sigma-Aldrich) to the experimental buffer. All stock solutions were stored at -20°C until used.

2.8 | Statistics

Values are reported as means \pm SEM, and n is the number of cells evaluated from N different experiments. For all comparisons Student's t -test for unpaired data was

applied and $P < 0.05$ was considered to be statistically significant.

3 | RESULTS

3.1 | Activation of TRPV4 produces opposite changes in V_m of WT- and AQP2-RCCD₁ cells without reflecting differences in $[\text{Ca}^{2+}]_i$ signals

To test the hypothesis that AQP2 can modulate SOCE by influencing the TRPV4-KCa interaction, our first step was to elucidate if AQP2 expression determines V_m kinetics upon TRPV4 activation on RCCD₁ cells. To accomplish this, we exposed WT- and AQP2-RCCD₁ cells to the specific TRPV4 activator 4 α -PDD (10 μM) while recording V_m with the voltage-sensitive fluorescent probe DIBAC₄(3). This dye has been widely used to reproducibly measure V_m under both depolarizing and hyperpolarizing conditions in a broad range of cells.^{25,26} WT- and AQP2-RCCD₁ cells show analogous V_m values in basal conditions and a comparable change under depolarizing conditions with a high extracellular K^+ solution (95 mM) (see section 2). Figure 2A shows that when WT-RCCD₁ cells were exposed to 4 α -PDD, a depolarization compatible with $\text{Ca}^{2+}/\text{Na}^+$ entry occurs. In contrast, a hyperpolarization was observed in AQP2-RCCD₁ cells. Figure 2B shows mean values of F_i/F_0 measured 10 min after 4 α -PDD treatment. It can be observed that, in both cell lines, the changes in V_m induced by the addition of 4 α -PDD disappear when incubating the cells with the selective TRPV4 antagonist HC-067047 (HC, 100 nM) demonstrating the participation of this channel. Then, we explored if the hyperpolarization observed in AQP2-RCCD₁ cells was due to the activation of a KCa channel. In the absence of extracellular Ca^{2+} no hyperpolarization occurs when TRPV4 was activated, supporting the idea that a KCa channel could be involved. The depolarization observed in this condition is probably due to the fact that Na^+ is entering through TRPV4 channels. Since in mouse CCD, SK3 channels (KCa 2.3) have recently been demonstrated to be functionally coupled with TRPV4 we pretreated cells with apamin (300 nM), a selective blocker of SK channels.^{20,27} Figure 2B shows that hyperpolarization disappears in the presence of apamin, confirming the participation of SK3 channel. Addition of apamin under basal conditions had no effect on resting V_m of AQP2-RCCD₁ cells (ΔV_m ($V_{m\text{ control}} - V_{m\text{ apamin}}$): 2.69 ± 3.7 mV, $n = 70$, $N = 3$, NS).

We next studied if AQP2 expression can shape $[\text{Ca}^{2+}]_i$ signaling patterns due to specific activation of TRPV4 with 4 α -PDD in isotonic conditions. Figure 2D shows the time course of the fluorescence ratios in 20 representative cells of both WT- and AQP2-RCCD₁ cells loaded with the membrane

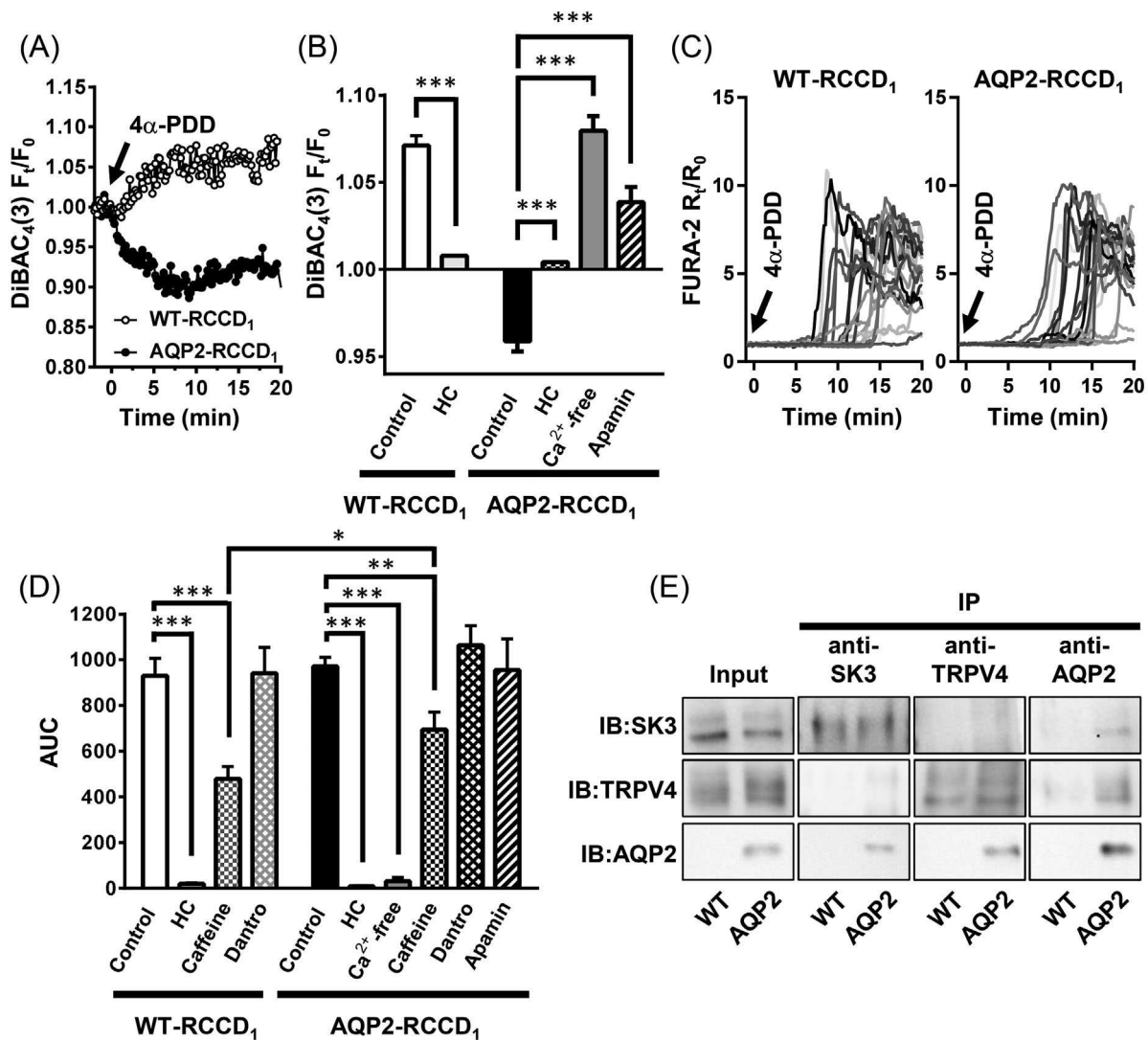


FIGURE 2 Vm and Ca²⁺ changes after 4 α -PDD treatment and co-immunoprecipitation studies in WT- and AQP2-RCCD₁ cells. A, Representative experiments showing the effect of 4 α -PDD (10 μ M) on Vm. Traces represent normalized fluorescence (F_t/F_0) changes measured using DiBAC₄(3). B, Bars represent F_t/F_0 measured 10 min after 4 α -PDD treatment. Quantitative analysis of identical protocols using specific inhibitors for TRPV4 (HC-067047, 100 nM) for SK channel (apamin, 300 nM) and a Ca²⁺-free solution. Values are the mean \pm SEM of at least 105 cells from three independent experiments, *** P < 0.001. C, Traces correspond to relative fluorescence ratios (R_t/R_0) of 20 representative cells measured using Fura-2. The arrow indicates the time point where cells were treated with 4 α -PDD (10 μ M) in control conditions. D, Quantitative analysis of Ca²⁺ signals using the area under the curve (AUC) during 20 min after TRPV4 activation in the same conditions as B and in the presence of caffeine (5 mM) or dantrolene (Dantrol, 10 μ M). Values are the mean \pm SEM of at least 255 cells from six independent experiments, *** P < 0.001, ** P < 0.01, * P < 0.05. E, Co-immunoprecipitation (IP) of SK3, AQP2, and TRPV4 in WT- and AQP2-RCCD₁ cell lysates. Immunoblots (IB) of SK3, TRPV4, and AQP2 were performed. The data are representative of three independent experiments

permeable ratiometric [Ca²⁺]_i indicator, Fura-2. The kinetics of TRPV4 activation is similar in AQP2 and WT-RCCD₁ cells. Surprisingly, the lag in Ca²⁺ response to 4 α -PDD was larger than the lag observed in Vm response. It has been proposed that opening of single or few TRP channels can evoke highly localized calcium signals (sparklets), particularly the opening of not more than four TRPV4 channels was found sufficient to evoke hyperpolarization and maximal endothelium-dependent dilation of mesenteric arteries.¹⁹ Therefore, it is likely that we are not able to detect, with

our measurement system, the initial highly localized [Ca²⁺]_i signals that trigger the Vm changes that we are measuring. Moreover, the changes in Vm and in [Ca²⁺]_i were abolished by HC in both cell lines showing the specificity of the response (Figure 2D). The quantification of Ca²⁺ entry was calculated as the area under the curve (AUC) during a period of 20 min after the application of 4 α -PDD (Figure 2D). WT- and AQP2-RCCD₁ cells show similar AUC values. Despite being highly dependent on extracellular Ca²⁺, [Ca²⁺]_i signals were not affected by Vm changes elicited by apamin

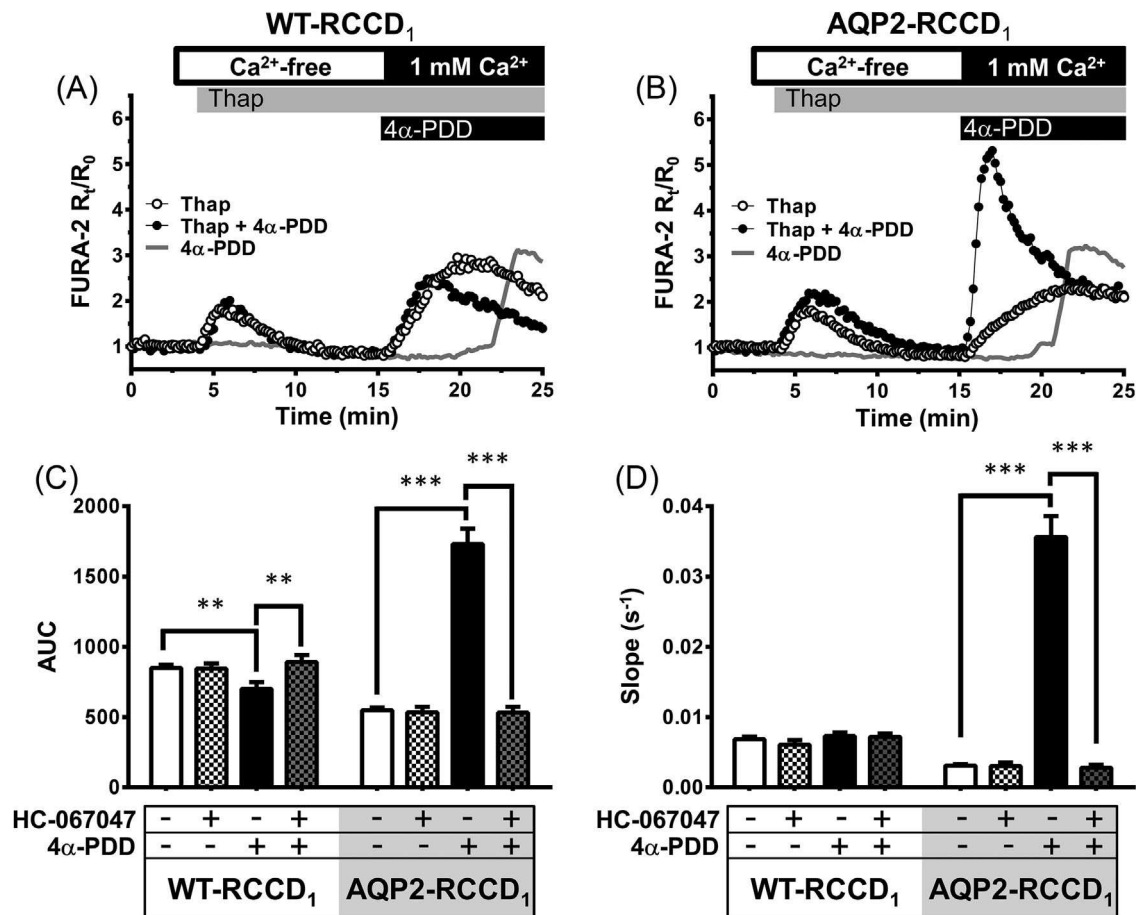


FIGURE 3 Differential SOCE response to 4 α -PDD in WT- and AQP2-RCCD₁ cells. A and B, Representative experiments of the relative fluorescence ratios of Fura-2 (R_i/R_0). A classic protocol to study SOCE was performed. WT- (A) and AQP2- (B) RCCD₁ cells were treated with 1 μ M Thap. in a Ca²⁺-free medium to induce store depletion. In these conditions Thap. induces a transient [Ca²⁺]_i increase (first peak) caused by store depletion. Re-addition of Ca²⁺ (1 mM) to the medium stimulates Ca²⁺ influx (second peak) from the extracellular medium (Thap., open symbols). In the same conditions the effect of 4 α -PDD in WT- and AQP2-RCCD₁ cells was tested (Thap. + 4 α -PDD, filled symbols). An identical protocol was realized using 4 α -PDD but avoiding the addition of Thap. to the medium (4 α -PDD, gray line). C and D, Area under the curve (AUC) during the first 10 min (C) and slope of [Ca²⁺]_i kinetics (D) in the first minute of Ca²⁺ influx of traces (second peak) shown in A and B. The effect of the specific inhibitor of TRPV4 (HC-067047) is also shown. Values are the mean \pm SEM of at least 105 cells from three independent experiments, ** P < 0.01, *** P < 0.001

treatment in AQP2-RCCD₁ cells. Therefore, although the activation of TRPV4 with 4 α -PDD in WT- and AQP2-RCCD₁ cells responds oppositely in changes in V_m , these differences are not reflected, at first glance, by changes in [Ca²⁺]_i. Probably Ca²⁺ entry by TRPV4 channels may activate the mechanism of Ca²⁺-induced Ca²⁺ release (CICR) from endoplasmic reticulum (ER) a process that is not affected by plasma membrane potential changes. To further examine this point, we performed experiments in the presence of caffeine or dantrolene. The incubation with caffeine (5 mM), an inhibitor of Ca²⁺ release from inositol triphosphate receptors (InsP3R)²⁸ significantly diminished the response in both cell lines (Figure 2D). On the contrary, TRPV4-mediated [Ca²⁺]_i signals were unaffected by

preincubation with dantrolene (Dantrol, 10 μ M), an inhibitor of Ca²⁺ release from ryanodine receptors (RyRs).²⁹ Altogether, these results suggest that TRPV4 activation triggers both Ca²⁺ influx and CICR in both cell lines. Nevertheless, when the CICR component was abolished, [Ca²⁺]_i signals were greater in AQP2-RCCD₁ cells evidencing a higher Ca²⁺ entry probably due to the hyperpolarization observed in AQP2-RCCD₁ cells. To test a possible physical association between AQP2, SK3 and TRPV4 proteins we performed co-immunoprecipitation studies. We found that an anti-AQP2 antibody could pull down TRPV4 and SK3 in cell lysates from AQP2-RCCD₁ cells. Furthermore, both anti-TRPV4 and anti-SK3 antibodies can reciprocally pull down AQP2. Neither anti-TRPV4 nor anti-SK3 antibodies were able to pull

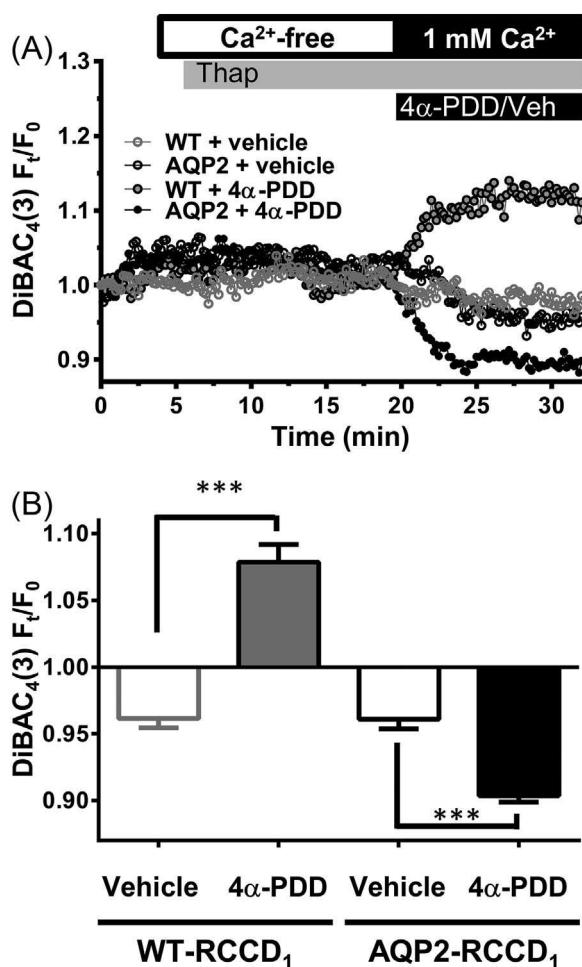


FIGURE 4 Changes in Vm during SOCE in WT- and AQP2-RCCD₁ cells. A, Representative experiments of the fluorescence measured using DiBAC₄(3) with the same protocol shown in Figure 3 either in the presence (+4α-PDD) or in the absence (+vehicle) of TRPV4 activation with 4α-PDD (10 μM). B, Bars represent mean ± SEM values of F_t/F_0 10 min after 4α-PDD or vehicle was added. Values are the mean ± SEM of at least 143 cells from four independent experiments, *** $P < 0.001$

down SK3 nor TRPV4 in WT and AQP2-RCCD₁ cells. These results provide clear evidence that TRPV4 and SK3 channels are physically coupled to AQP2 forming a functional complex. Thus, despite both cell lines express SK3 and TRPV4 channels, SK3 is only activated by TRPV4 in AQP2-RCCD₁ cells.

3.2 | Modulation of SOCE by TRPV4 and SK channels depends on AQP2 expression

Since Ca²⁺ entry through store-operated Ca²⁺ channels (SOC) is an electrogenic process driven by chemical and electrical forces, Vm can regulate SOCE such that less Ca²⁺ enters upon depolarization and membrane hyperpolarization

promotes Ca²⁺ influx.³⁰ Because opposite changes in Vm were observed in the presence or absence of AQP2 in RCCD₁ cells upon TRPV4 stimulation, we hypothesized that 4α-PDD could influence SOCE in an AQP2 dependant manner. Figure 3A (WT-RCCD₁) and 3B (AQP2-RCCD₁) show representative experiments of the “Ca²⁺ re-addition protocol,” where store depletion is first induced by adding 1 μM thapsigargin (Thap.) in a Ca²⁺ free solution, followed by reintroduction of extracellular Ca²⁺ to quantify SOCE.³⁰ Under activation of TRPV4 with 4α-PDD, SOCE was reduced in WT-RCCD₁ cells and considerably increased in AQP2 expressing cells. These kinetics were also compared with the time course of the response to 4α-PDD in the absence of Thap. (gray line). It can be observed that in this condition the increase of Ca²⁺ due to the activation of TRPV4 occurs with a delay similar to that observed in Figure 2.

The extent of SOCE activity was calculated as areas under the curves (AUC) during the first 10 min, following Ca²⁺ re-addition and the slope was calculated from the first minute after Ca²⁺ re-addition. The TRPV4 agonist considerably increased AUC and the slope in AQP2-expressing cells (Figures 3C and 3D). In contrast, WT-RCCD₁ cells showed a slight decreased AUC and the slope did not change (Figures 3C and 3D). In both cell lines HC had no effect on basal SOCE but significantly inhibited the effects of 4α-PDD on SOCE.

We then measured Vm kinetics during SOCE both in TRPV4 stimulated and unstimulated conditions. Figure 4 shows that SOCE produces a small hyperpolarization in both cell lines as it is reported for many other systems.^{31,32} However, when TRPV4 was stimulated with 4α-PDD, AQP2-expressing cells hyperpolarization was considerably enhanced and WT-RCCD₁ cells depolarize as in basal conditions (see Figure 2).

To investigate if SK channels are involved in the increase of SOCE observed under TRPV4 activation in AQP2-RCCD₁ cells, we tested the effect of apamin. Figure 5 shows representative experiments of the effect of apamin in SOCE control (Figure 5A) and under TRPV4 stimulation (Figure 5B). Apamin had no effect on control SOCE but significantly reduces AUC and the slope of SOCE when TRPV4 was activated with 4α-PDD (Figures 5C and 5D). These results support the idea that SK channels are involved in this process. We also tested the SOCE inhibitor SKF-96365 (20 μM) in SOCE control and under TRPV4 stimulation (Figures 5C and 5D). SKF-96365 significantly reduced [Ca²⁺]_i rises in control SOCE. Interestingly, when SKF-96365 was present, SOCE was unmodified by TRPV4 activation in AQP2-expressing cells. Altogether, these results allow us to propose that SOCE can be increased by TRPV4 activation by a mechanism that depends on AQP2 expression and also, at least partially, on an apamin sensitive SK channel.

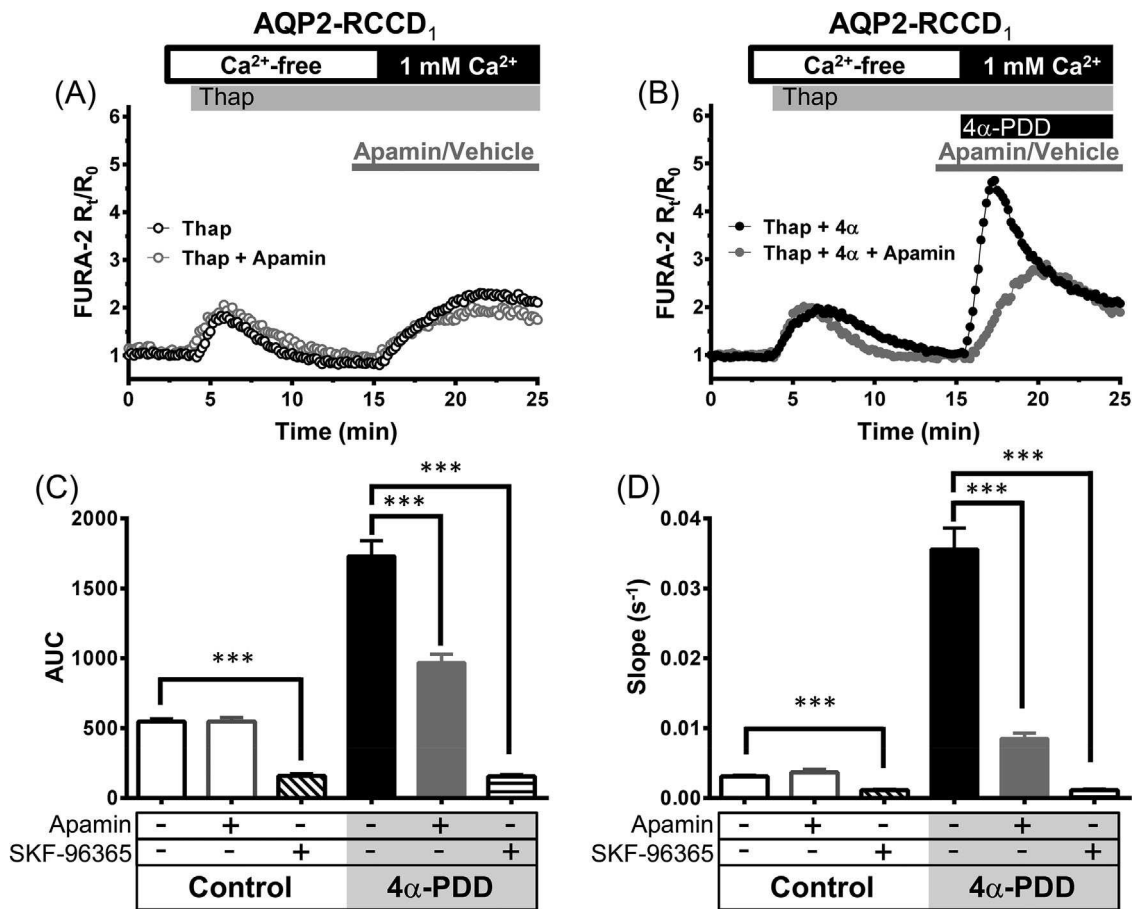


FIGURE 5 Effect of apamin and SKF-96365 on SOCE in AQP2-RCCD₁ cells. A and B, Representative experiments measured using Fura-2 of the classic protocol to study SOCE in control conditions (Thap.) or in cells treated with apamin (300 nM) (Thap. + Apamin) (A). Representative experiments using the same protocol shown in A, but in the presence of 4α-PDD (B). C and D, Quantitative analysis of different parameters of traces shown in A and B and with the SOCE inhibitor SKF-96365 (20 μM): area under the curve (AUC) in the first 10 min (C) and slope of [Ca²⁺]_i kinetics in the first minute of Ca²⁺ entry (D). Values are the mean ± SEM of at least 143 cells from five independent experiments, ****P* < 0.001

3.3 | AQP2 colocalizes with SK3 and, after store depletion, also with TRPV4

Since in a previous study we revealed that hypotonic stimulation enriched TRPV4 only in the membrane of AQP2-RCCD₁⁹ we tested if store depletion can have similar consequences. We performed immunofluorescence confocal analysis on WT- and AQP2-RCCD₁ cells co-stained with the selective fluorescent plasma membrane marker WGA-488 (green) and with anti-TRPV4 (red). Merge of single plane confocal images demonstrates a higher overlapping of TRPV4 staining with the plasma membrane only in AQP2 expressing cells pretreated with Thap. (1 μM for 10 min) (Figure 6). Moreover, we quantified colocalization using Pearson's correlation coefficient (PCC) in WT- and AQP2-RCCD₁ cells pretreated either with Thap. or vehicle (DMSO). Obtained PCC values for store depleted AQP2

cells were the only ones statistically different from zero (0.15 ± 0.04 $n = 12$, $P < 0.01$). These experiments demonstrate that when stores were emptied TRPV4 could be translocated to the plasma membrane only in cells that express AQP2. We next investigated if AQP2 colocalizes with SK3 and/or with TRPV4 after treatment with Thap. + 4α-PDD. Figure 7A shows that, after treatment, there is an increase in TRPV4-AQP2 colocalization in the plasma membrane. Figure 7B shows that SK3 displayed both intracellular and plasma membrane staining and colocalization with AQP2 at the apical plasma membrane in both control and treated cells.

Together, our results suggest that AQP2 influences the localization/function of SK3 and TRPV4 channels. Hence, the activation of TRPV4 in AQP2-RCCD₁ cells determines V_m dynamics with consequences in the magnitude of SOCE transients.

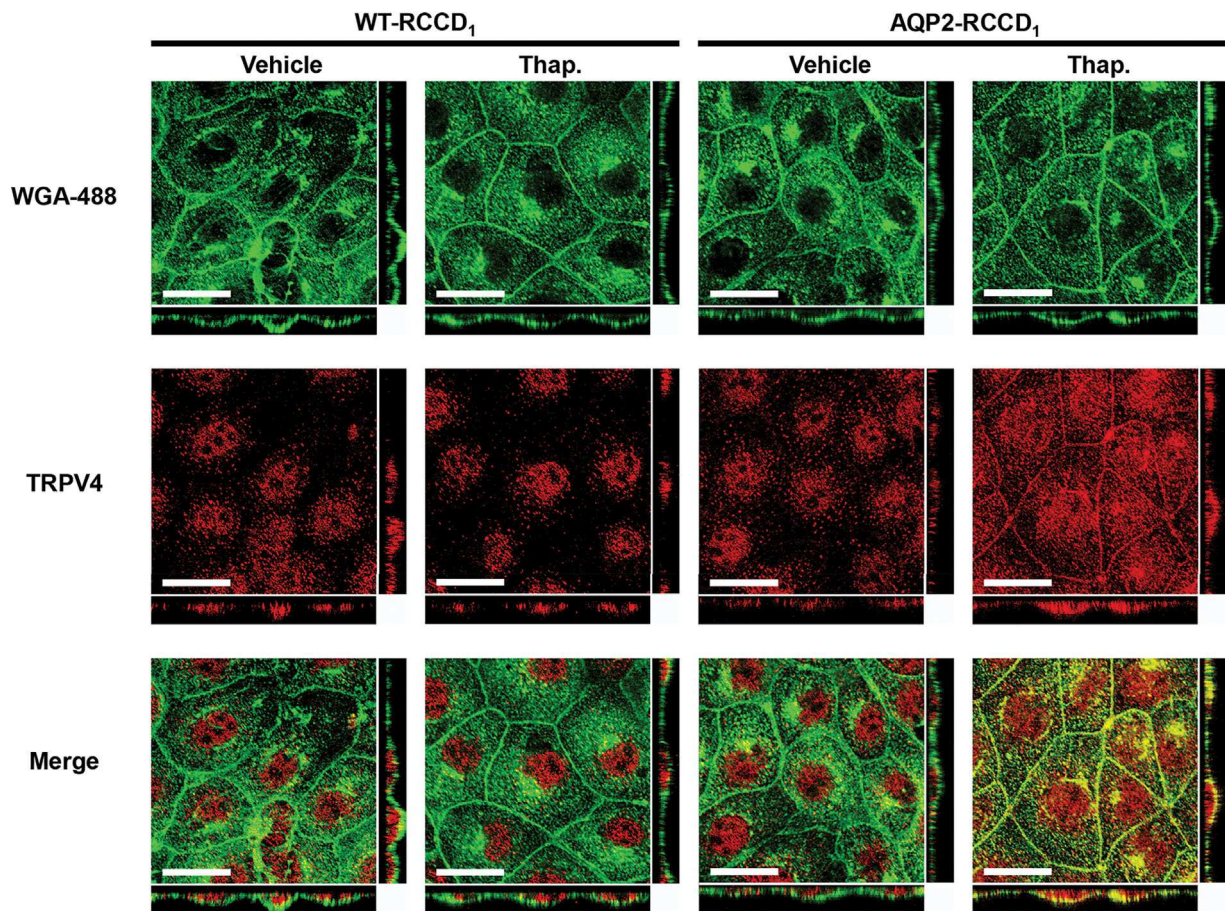


FIGURE 6 Store depletion induces TRPV4 translocation to the plasma membrane in AQP2-RCCD₁ cells. Confocal images showing a single xy plane and a cross section of xz and yz planes of WT- and AQP2-RCCD₁ cells incubated for 10 min with either vehicle (DMSO) or with Thap. (1 μM). Immunofluorescence experiments performed using a primary anti-TRPV4 antibody and a secondary Cy3-antibody (red) and WGA-488 (green). Scale bars: 30 μm

4 | DISCUSSION

In the present study we showed, for the first time in renal cells, that changes in V_m associated with TRPV4 activation depend on the expression of AQP2. In particular, AQP2 expression facilitates an apamin sensitive K^+ channel activation leading to a hyperpolarization of the cell membrane, impacting in SOCE. The specific activation of TRPV4 has been described in the literature as producing either hyperpolarization or depolarization of V_m . For instance, Konno et al³³ showed, in microglia, that opening of TRPV4 channels with 4 α -PDD induced membrane depolarization decreasing SOCE. They proposed that depolarization, in response to opening of the TRPV4 channel, attenuate the driving force for extracellular Ca^{2+} entry and suppress microglial activation, reducing the production of proinflammatory mediators. Conversely in different arteries and in mouse CCD, activation of TRPV4 hyperpolarized the plasma membrane^{20,34,35} but the impact in SOCE has not yet been investigated. The hyperpolarization was attributed to the fact that the influx of Ca^{2+} via TRPV4

channels led to the local activation of one or more KCa channels.^{17,18} Results of several works demonstrated that TRPV4 may be functionally linked to different KCa channels depending on animal species.^{19,36,37} In mouse aortic endothelial cells, TRPV4 is predominantly coupled to IK1 (KCa3.1)¹⁹ whereas in rat mesenteric artery TRPV4 is mainly coupled to SK3.³⁷ Our observation that 4 α -PDD elicits an SK channel activation in AQP2-RCCD₁ cells is in line with a study in CCD tubules of the mouse kidney where a functional coupling between TRPV4 and SK3 has been described.²⁰ This study also demonstrated that TRPV4 activates a BK channel. In our experiments, although apamin entirely abolishes the hyperpolarization, we cannot completely rule out a potential role of other KCa channels. Until recently, BK and ROMK (the renal outer medullary potassium channel) were believed to solely govern the secretory efflux of K^+ across the apical membrane of CCD cells. However, the recent discovery that SK3 is functionally expressed in the mouse distal nephron in CCD, raised the possibility that SK3 may be a key pathway for Ca^{2+} dependent regulation of V_m and K^+ secretion.^{20,27,38}

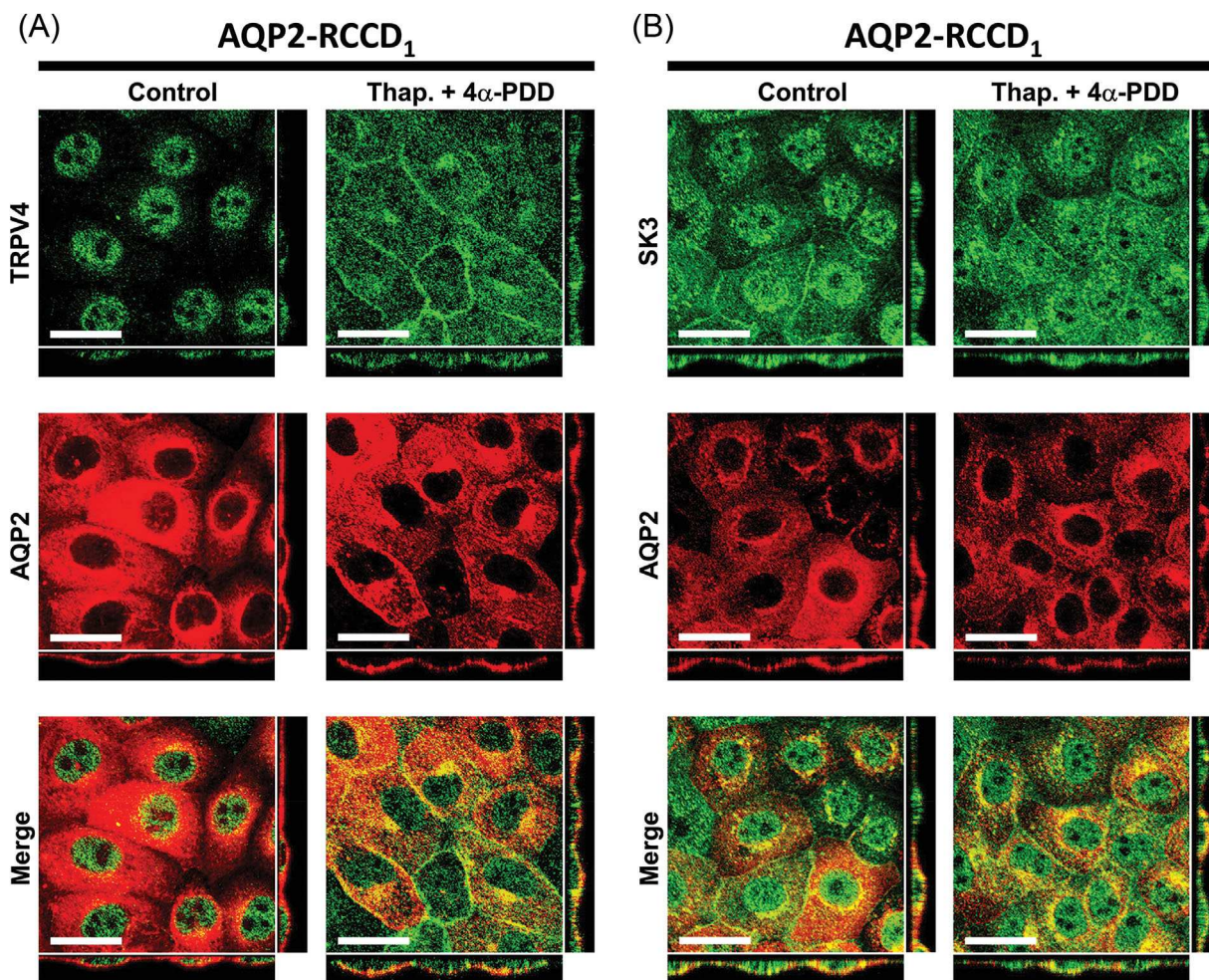


FIGURE 7 Colocalization of AQP2 with TRPV4 and SK3. Confocal images showing a single xy plane and a cross section of xz and yz planes of AQP2-RCCD₁ cells incubated for 5 min with either vehicle (DMSO) or with Thap. (1 μM) + 4α-PDD (10 μM). A, Immunofluorescence experiments performed using a primary anti-TRPV4 antibody and a secondary Alexa 488-antibody (green) and anti-AQP2 antibody and a secondary Alexa 568-antibody (red). B, Immunofluorescence experiments performed using a primary anti-SK3 antibody and a secondary Alexa 488-antibody (green) and anti-AQP2 antibody and a secondary Alexa 568-antibody (red). Scale bars: 30 μm

To our knowledge our work is the first one showing SK3 expression, function and co-immunoprecipitation with AQP2 channel in rat CCD cells.

Although hyperpolarization due to K⁺ efflux should theoretically increase the driving force for Ca²⁺ entry, KCa activation has been reported to either enhance or have no impact at all on Ca²⁺ entry.^{34,39–41} Here, we show that [Ca²⁺]_i transients elicited only by TRPV4 activation do not reflect the different V_m changes seen in WT and AQP2-expressing cells in the same condition (Figure 2). This could be explained by the fact that Ca²⁺ entry by TRPV4 channels activate the mechanism of Ca²⁺-induced Ca²⁺ release (CICR) from endoplasmic reticulum (ER).^{36,42} Since Ca²⁺ release from ER should not be affected by plasma membrane V_m changes,⁴³ differences in Ca²⁺ influx by TRPV4 can be disguised. Consequently, the inhibitory effect of apamine on the hyperpolarization produced by TRPV4 activation was not reflected in a decrease in [Ca²⁺]_i. In line with this, our

experiments show that when CICR is inhibited with caffeine, Ca²⁺ influx is higher in AQP2 than in WT-RCCD₁ cells (Figure 2D). Interestingly, when Ca²⁺ stores were previously emptied, the TRPV4 mediated V_m changes were clearly reflected in SOCE (SOCE increases in hyperpolarized AQP2 cells and decreases in depolarized WT cells, Figures 3 and 4). Pretreatment of cells with apamin only modulates SOCE when TRPV4 is activated, suggesting that SK channels do not influence basal SOCE but are a key component of TRPV4-mediated SOCE modulation. Additionally, the increase of SOCE under TRPV4 activation disappears in the presence of the SOCE inhibitor, SKF96365. These results lead us to propose that, in AQP2 expressing cells, TRPV4 is acting upstream of the channels that mediate SOCE probably in part due to a gain in the driving force as a result of SK channels activation.

Three decades ago, SOCE was identified as a unique mechanism for Ca²⁺ entry through plasma membrane. The

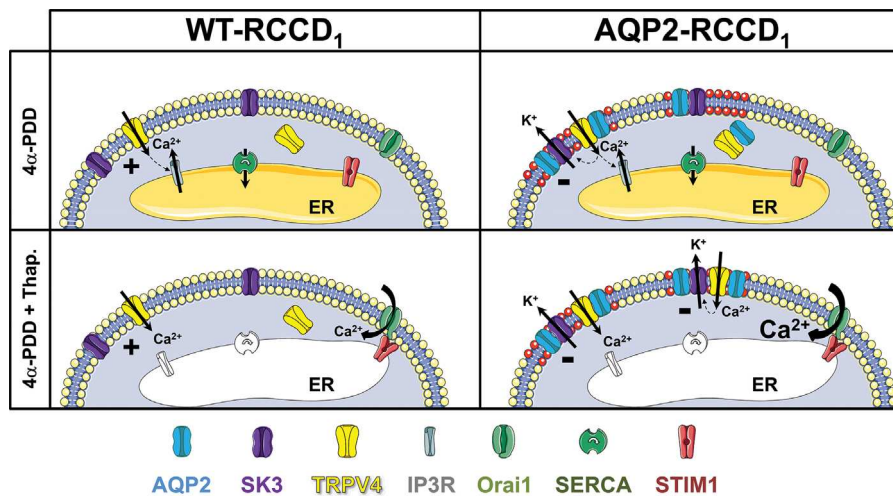


FIGURE 8 Schematic representation depicting the different responses to TRPV4 activation in WT- and AQP2-RCCD₁ cells. The activation of TRPV4 with 4 α -PDD increases [Ca²⁺]_i by Ca²⁺ entry and by triggering CICR from endoplasmic reticulum (ER) in both cell lines. The Ca²⁺ entry depolarizes (+) the plasma membrane in WT cells but hyperpolarizes (-) the plasma membrane in AQP2-RCCD₁ cells by stimulating the calcium-activated potassium channel SK3. This could be possible because of the proximity between AQP2-TRPV4 and AQP2-SK3 complexes in plasma membrane microdomains. When activating TRPV4, once the deposits were previously emptied with thaps., the plasma membrane microdomains are enriched with TRPV4 only in AQP2-RCCD₁ cells, favoring the hyperpolarization and then increasing the driving force for SOCE

presence of a variety of store-operated currents with different biophysical features described in the subsequent years suggested that the channel conducting SOCE was not unique.⁴⁴ In the last years, two key molecules playing crucial roles in SOCE regulation were discovered: the ER Ca²⁺ sensor protein STIM1, and the store-operated Ca²⁺ channel component Orai1. While the contribution of some TRPC channels to SOCE has been demonstrated,⁴⁵ the participation of TRPV4 on SOCE is controversial. Although some authors propose that TRPV4 does not participate in SOCE, others found that TRPV4 contributes to SOCE.^{46,47} Ma et al⁴⁷ demonstrated that Ca²⁺ store depletion stimulates the insertion of TRPV4-TRPC1 heteromeric channels into the plasma membrane, resulting in an increased Ca²⁺ influx in response to flow in a STIM1- and Orai1-dependent manner. These authors also show that TRPV4, TRPC1, and KCa1.1 form a physical complex in mammary arteries and that 11, 12-EETs and 4 α -PDD act through this complex to induce membrane hyperpolarization leading to vascular relaxation.^{35,47}

In the present work, we found that in basal conditions AQP2 and TRPV4 co-immunoprecipitate. However, AQP2 is mainly expressed at the plasma membrane and TRPV4 in the intracellular compartment, making it difficult to visualize a colocalization signal. Our studies measuring [Ca²⁺]_i and V_m shows that TRPV4 is consistently activated when we expose cells to 4 α -PDD showing that there is functional TRPV4 at the plasma membrane. In addition, we found that after treating cells with thapsigargin, TRPV4 is translocated to the plasma membrane only in cells that express AQP2. Moreover, after store depletion TRPV4 colocalizes with AQP2. In a previous

work we described a critical role of AQP2 in the translocation of TRPV4 to the cell membrane under a hypotonic shock, however, in this case the colocalization was not evident.⁹ Recently Shin et al⁴⁸ described that the formation of a complex between TRPV4 and STIM1 plays a crucial role in routing TRPV4 to the plasma membrane from the ER. In RCCD₁ cells, AQP2 could be influencing the interaction between STIM1 and TRPV4, enabling the trafficking of TRPV4 to the plasma membrane after store depletion. Future studies are necessary to investigate this signaling pathway.

In the current work, we also demonstrate that AQP2 co-immunoprecipitates and colocalizes with SK3 independently of store depletion. It has been proposed that KCa and Ca²⁺ permeable cation channels may be clustered in localized positions within the cell membrane to form functional units and that caveolae may constitute the scaffolding for such microcompartmental organization. Particularly, it has been described in caveolae of endothelial cells a dynamic microcompartmentation of Cav-1, TRPV4, and SK3 with functional implications.⁴⁹ In renal cells it has been previously demonstrated that AQP2 colocalizes with caveolin-1 at caveolar structures on the apical plasma membrane.⁵⁰ Our result that SK3 and TRPV4 did not co-immunoprecipitate despite AQP2 co-immunoprecipitate with SK3 and with TRPV4 could be explained by the fact that two populations of AQP2 coexist: one that interacts with TRPV4 and another that interacts with SK3. One possibility is that parts of both complexes are localized at a plasma membrane microdomain (for example caveolar structures or lipid rafts). When cells are treated with thapsigargin + 4 α -PDD there is an increase in quantity of AQP2-TRPV4 at this microdomain potentiating

the functional interaction between SK3 and TRPV4. Figure 8 shows a possible model that fits our principal findings. Further studies are needed to understand the mechanisms governing the compartmentalization into microdomains of these proteins and the possible role of AQP2 in this macromolecular complex.

Little is known about the role of SOCE in normal renal function or disease. Recently Mamenko et al²¹ demonstrated, in freshly isolated split-open CDs, that SOCE plays an important role in AVP induction of AQP2 translocation to the apical plasma membrane. In the presence of AVP water reabsorption requires not only high levels of AQP2 at the plasma membrane but also an osmotic gradient. Hypotonicity is a well-known TRPV4 activation factor. Thus, our results in AQP2-expressing cells showing that TRPV4 activation increases SOCE, and Mamenko's findings demonstrating that SOCE regulates AVP-induced AQP2 membrane expression let us propose the existence of a local control mechanism. Most probably, when AVP circulating levels increase AQP2 shuttle to the apical membrane, TRPV4 activation by hypotonic fluid can enhance SOCE, an effect that, in turn, would potentiate AVP-induced AQP2 membrane expression. This mechanism may be important for rapid adjustments in renal free water handling. In the cells of the cortical collecting duct, this mechanism would self-limiting as water is reabsorbed and the luminal fluid becomes isotonic, disappearing the stimulus for the activation of TRPV4.

In summary, this study demonstrates, for the first time, that AQP2 co-immunoprecipitates with SK3 and TRPV4 forming a functional complex that seems to be crucial for the activation of SK3 channels by TRPV4 in collecting duct cells. We also reveal that the hyperpolarization resulting from the activation of SK channel modulates the magnitude of SOCE. Moreover, in AQP2-RCCD₁ cells, AQP2 colocalizes with SK3 and after store depletion, also with TRPV4. These findings open the perspective to further investigate whether the interplay between different AQPs with TRPV4 and K_{Ca} channels can be an important mechanism to modulate SOCE with physiological relevance.

ACKNOWLEDGMENTS

The authors thank N. Beltramone and M. Fanelli for technical assistance, L. Galizia for helpful discussion and G. Bartolomé for providing language help.

ORCID

Alejandro Pizzoni  <http://orcid.org/0000-0002-7714-9968>
 Valeria Rivarola  <http://orcid.org/0000-0002-8879-1198>
 Claudia Capurro  <http://orcid.org/0000-0002-6374-7369>
 Paula Ford  <http://orcid.org/0000-0002-3656-0806>

REFERENCES

- Galán-Cobo A, Ramírez-Lorca R, Echevarría M. Role of aquaporins in cell proliferation: what else beyond water permeability? *Channels*. 2016;10:185–201.
- Kitchen P, Day R, Salman M, Conner M, Bill R, Conner A. Beyond water homeostasis: diverse functional roles of mammalian aquaporins. *BBA Gen Subj*. 2015;1850:2410–2421.
- Hill A, Shachar-Hill Y. Are aquaporins the missing transmembrane osmosensors? *J Membr Biol*. 2015;248:753–765.
- Liu X, Bandyopadhyay B, Nakamoto T, et al. Role for AQP5 in Activation of TRPV4 by Hypotonicity: concerted involvement of AQP5 and TRPV4 in regulation of cell volume recovery. *J Biol Chem*. 2006;281:15485–15495.
- Galizia L, Flamenco M, Rivarola V, Capurro C, Ford P. Role of AQP2 in activation of calcium entry by hypotonicity: implications in cell volume regulation. *Am J Physiol Renal Physiol*. 2008;294:F582.
- Pasantes-Morales H, Morales Mulia S. Influence of calcium on regulatory volume decrease: role of potassium channels. *Nephron*. 2000;86:414–427.
- Mola MG, Sparaneo A, Gargano CD, et al. The speed of swelling kinetics modulates cell volume regulation and calcium signaling in astrocytes: a different point of view on the role of aquaporins. *Glia*. 2016;64:139–154.
- Benfenati V, Caprini M, Dovizio M, et al. An aquaporin-4/transient receptor potential vanilloid 4 (AQP4/TRPV4) complex is essential for cell-volume control in astrocytes. *Proc Natl Acad Sci USA*. 2011;108:2563–2568.
- Galizia L, Pizzoni A, Fernandez J, Rivarola V, Capurro C, Ford P. Functional interaction between AQP2 and TRPV4 in renal cells. *J Cell Biochem*. 2012;113:580–589.
- Jo A, Ryskamp D, Phuong T. TRPV4 and AQP4 channels synergistically regulate cell volume and calcium homeostasis in retinal muller glia. *J Neurosci*. 2015;35:13525–13537.
- Parekh A, Putney J. Store-operated calcium channels. *Physiol Rev*. 2005;85:757–810.
- Di Giusto G, Flamenco P, Rivarola V, et al. Aquaporin 2-increased renal cell proliferation is associated with cell volume regulation. *J Cell Biochem*. 2012;113:3721–3729.
- Lee WH, Choong LY, Mon NN, et al. TRPV4 regulates Breast cancer cell extravasation, stiffness and actin cortex. *Sci Rep*. 2016;6:27903.
- White J, Cibelli M, Urban L, Nilius B, Mc Geown J, Nagy I. TRPV4: molecular conductor of a diverse orchestra. *Physiol Rev*. 2016;96:911–973.
- Rivarola V, Flamenco P, Melamud L, Galizia L, Ford P, Capurro C. Adaptation to alkalosis induces cell cycle delay and apoptosis in cortical collecting duct cells: role of aquaporin-2. *J Cell Physiol*. 2010;224:405–413.
- Taniguchi J, Tsuruoka S, Mizuno A, Sato J, Fujimura A, Suzuki M. TRPV4 as a flow sensor in flow-dependent K⁺ secretion from the cortical collecting duct. *Am J Physiol Renal Physiol*. 2006;292:F667.
- Arnhold S, Goletz I, Klein H, et al. Isolation and characterization of bone marrow-derived equine mesenchymal stem cells. *Am J of Vet Res*. 2007;68:1095–1105.
- Gao F, Wang D. Hypotension induced by activation of the transient receptor potential vanilloid 4 channels: role of Ca²⁺-activated K⁺ channels and sensory nerves. *J Hypertens*. 2010;28:102–110.

19. Sonkusare S, Bonev A, Ledoux J, et al. Elementary Ca^{2+} signals through endothelial TRPV4 channels regulate vascular function. *Science*. 2012;336:597–601.
20. Berrou J, Mamenko M, Zaika O, et al. Emerging role of the calcium-Activated, small conductance, SK3 K^+ channel in distal tubule function: regulation by TRPV4. *PLoS ONE*. 2014;9:e95149.
21. Mamenko M, Dhande I, Tomilin V, et al. Defective store-operated calcium entry causes partial nephrogenic diabetes insipidus. *J Am Soc Nephrol*. 2015;27:2035–2048.
22. Blot-Chabaud M, Laplace M, Cluzeaud F, et al. Characteristics of a rat cortical collecting duct cell line that maintains high trans-epithelial resistance. *Kidney Int*. 1996;50:367–376.
23. Capurro C, Rivarola V, Kierbel A, et al. Vasopressin regulates water flow in a rat cortical collecting duct cell line not containing known aquaporins. *J Mem Biol*. 2001;179:63–70.
24. Ford P, Rivarola V, Chara O, et al. Volume regulation in cortical collecting duct cells: role of AQP2. *Biol Cell*. 2005;97:687–697.
25. Balghi H, Robert R, Rappaz B, et al. Enhanced Ca^{2+} entry due to Orai1 plasma membrane insertion increases IL-8 secretion by cystic fibrosis airways. *FASEB J*. 2011;25:4274–4291.
26. Fernández J, Di Giusto G, Kalstein M, et al. Cell volume regulation in cultured human retinal Müller cells is associated with changes in transmembrane potential. *PLoS ONE*. 2013;8:57268.
27. Jin M, Berrou J, Chen L, O'Neil R. Hypotonicity-induced TRPV4 function in renal collecting duct cells: modulation by progressive cross-talk with Ca^{2+} -activated K^+ channels. *Cell Calcium*. 2012;51:131–139.
28. Kang SS, Han KS, Ku BM, et al. Inhibition of the Ca^{2+} release channel, IP_3R subtype 3 by caffeine slows glioblastoma invasion and migration and extends survival. *Cancer Res*. 2010;70:1173–1183.
29. Thomas NL, Williams AJ. Pharmacology of ryanodine receptors and Ca^{2+} -induced Ca^{2+} release. *WIREs Membr Transp Signal*. 2012;1:383–397.
30. Bird G, DeHaven W, Smyth J, Putney J. Methods for studying store-operated calcium entry. *Methods*. 2008;46:204–212.
31. Darbellay B, Arnaudeau S, König S, et al. STIM1- and orai1-dependent store-operated calcium entry regulates human myoblast differentiation. *J Biol Chem*. 2008;284:5370–5380.
32. Song K, Zhong X, Xia X, et al. Orai1 forms a signal complex with SK3 channel in gallbladder smooth muscle. *Biochem Biophys Res Comm*. 2015;466:456–462.
33. Konno M, Shirakawa H, Iida S, et al. Stimulation of transient receptor potential vanilloid 4 channel suppresses abnormal activation of microglia induced by lipopolysaccharide. *Glia*. 2012;60:761–770.
34. Lin M, Jian M, Taylor M, et al. Functional coupling of TRPV4, IK, and SK channels contributes to Ca^{2+} -dependent endothelial injury in rodent lung. *Pulm Circ*. 2015;5:279–290.
35. Ma Y, Zhang P, Li J, et al. Epoxyeicosatrienoic acids act through TRPV4-TRPC1-KCa1.1 complex to induce smooth muscle membrane hyperpolarization and relaxation in human internal mammary arteries. *BBA-Mol Bas Dis*. 2015;1852:552–559.
36. Earley S, Heppner T, Nelson M, Brayden J. TRPV4 forms a novel Ca^{2+} signaling complex with ryanodine receptors and BKCa channels. *Circ Res*. 2005;97:1270–1279.
37. Ma X, Du J, Zhang P, et al. Functional role of TRPV4-KCa2.3 signaling in vascular endothelial cells in normal and streptozotocin-Induced diabetic rats. *Hypertension*. 2013;62:134–139.
38. Li Y, Hu H, Butterworth M, Tian J, Zhu M, O'Neil R. Expression of a diverse array of Ca^{2+} -Activated K^+ channels (SK1/3, IK1, BK) that functionally couple to the mechanosensitive TRPV4 channel in the collecting duct system of kidney. *PLoS ONE*. 2016;11:0155006.
39. Hoebel B, Kostner G, Graier W. Activation of microsomal cytochrome P450 mono-oxygenase by Ca^{2+} store depletion and its contribution to Ca^{2+} entry in porcine aortic endothelial cells. *Br J Pharmacol*. 1997;121:1579–1588.
40. Fleming I, Rueben A, Popp R, et al. Epoxyeicosatrienoic acids regulate Trp channel dependent Ca^{2+} signaling and hyperpolarization in endothelial cells. *Arterioscler Thromb Vasc Biol*. 2007;27:2612–2618.
41. Cohen K, Jackson W. Membrane hyperpolarization is not required for sustained muscarinic agonist-Induced increases in intracellular Ca^{2+} in arteriolar endothelial cells. *Microcirculation*. 2010;12:169–182.
42. Dunn K, Hill-Eubanks D, Liedtke W, Nelson M. TRPV4 channels stimulate Ca^{2+} -induced Ca^{2+} release in astrocytic endfeet and amplify neurovascular coupling responses. *Proc Natl Acad Sci USA*. 2013;110:6157–6162.
43. Penner R, Matthews G, Neher E. Regulation of calcium influx by second messengers in rat mast cells. *Nature*. 1988;334:499–504.
44. Lopez J, Albarán L, Gómez L, Smani T, Salido G, Rosado J. Molecular modulators of store-operated calcium entry. *BBA Mol Cell Res*. 2016;1863:2037–2043.
45. Pani B, Ong H, Brazer S, et al. Activation of TRPC1 by STIM1 in ER-PM microdomains involves release of the channel from its scaffold caveolin-1. *Proc Natl Acad Sci USA*. 2009;106:20087–20092.
46. Lorenzo I, Liedtke W, Sanderson M, Valverde M. TRPV4 channel participates in receptor-operated calcium entry and ciliary beat frequency regulation in mouse airway epithelial cells. *Proc Natl Acad Sci USA*. 2008;105:12611–12616.
47. Ma X, Cheng K, Wong C, et al. Heteromeric TRPV4-C1 channels contribute to store-operated Ca^{2+} entry in vascular endothelial cells. *Cell Calcium*. 2011;50:502–509.
48. Shin S, Lee E, Chun J, Hyun S, Kang S. Phosphorylation on TRPV4 serine 824 regulates interaction with STIM1. *Open Biochem J*. 2015;9:24–33.
49. Goedicke-Fritz S, Kaistha A, Kacik M, et al. Evidence for functional and dynamic microcompartmentation of Cav-1/TRPV4/K(Ca) in caveolae of endothelial cells. *Eur J Cell Biol*. 2015;94:391–400.
50. Aoki T, Suzuki T, Hagiwara H, et al. Close association of aquaporin-2 internalization with caveolin-1. *Acta Histochem Cytochem*. 2012;45:139–146.

How to cite this article: Pizzoni A, López González M, Di Giusto G, Rivarola V, Capurro C, Ford P. AQP2 can modulate the pattern of Ca^{2+} transients induced by store-operated Ca^{2+} entry under TRPV4 activation. *J Cell Biochem*. 2017;1–14.
<https://doi.org/10.1002/jcb.26612>